Nonlinear Dynamics **17:** 269–284, 1998.

Control of Chaotic Motion in a Spinning Spacecraft with a Circumferential Nutational Damper

P. A. MEEHAN* and S. F. ASOKANTHAN
Department of Mechanical Engineering, University of Queensland, Brisbane, Qld. 4072, Australia

(Received: 3 September 1996; accepted: 15 December 1997)

Abstract. Control of chaotic vibrations in a simplified model of a spinning spacecraft with a circumferential nutational damper is achieved using two techniques. The control methods are implemented on a realistic spacecraft parameter configuration which has been found to exhibit chaotic instability when a sinusoidally varying torque is applied to the spacecraft for a range of forcing amplitude and frequency. Such a torque, in practice, may arise in the platform of a dual-spin spacecraft under malfunction of the control system or from an unbalanced rotor or from vibrations in appendages. Chaotic instabilities arising from these torques could introduce uncertainties and irregularities into a spacecraft's attitude and consequently could have disastrous affects on its operation. The two control methods, recursive proportional feedback (RPF) and continuous delayed feedback, are recently developed techniques for control of chaotic motion in dynamical systems. Each technique is outlined and the effectiveness of the two strategies in controlling chaotic motion exhibited by the present system is compared and contrasted. Numerical simulations are performed and the results are studied by means of time history, phase space, Poincaré map, Lyapunov characteristic exponents and bifurcation diagrams.

Keywords: Chaos, control, spacecraft, bifurcations.

1. Introduction

A number of investigations into spinning spacecraft stability have been performed in the recent past after abnormalities were observed in dual-spin spacecraft in practice. Many of these observed instabilities have been attributed to excitations from structural imperfections in combination with the inherent nonlinear dynamics of the system. Many researchers, amongst others [1–3], have investigated the attitude stability and behaviour of a dual-spin spacecraft due to parametric fluctuations resulting from structural imperfections. The results obtained in the above studies are of concern to designers since a spacecraft may pass through these instability regions during rotor spin-up or during a malfunction such as run-down of the momentum wheel during temporary power loss. However, very little attention has been concentrated on investigating chaotic instabilities that can arise in a spacecraft system. This paper extends the understanding of this form of instabilities in spacecraft systems by investigating possible strategies to quench these instabilities.

Moon [4] describes a large range of simple mechanical and electrical systems that are known to exhibit chaotic vibrations, however, it has been only recently that chaotic motion has been investigated in spacecraft configurations. Both Holmes and Marsden [5] and Koiller [6] have performed analyses on configurations similar to that of a dual-spin satellite using Melnikov's method to show the existence of horseshoes. Piper and Kwatny [7] have also investigated a commonly used momentum exchange spacecraft attitude control configuration

* Present address: Industrial Automation Services, P.O. Box 100, Teralba, 2284, Australia.

and have shown the existence of multiple limit cycles and strange attractors for a range of motor time constants. Gray et al. [8] have also provided analytical results for the prediction of chaotic motion in a single body spacecraft with a viscous damper during an attitude transition manoeuvre. These results are of importance to spacecraft designers as any instabilities in the attitude dynamics of a spacecraft could have disastrous effects on its normal operation. For example, chaotic motion in the attitude motion of a communication satellite would be seriously detrimental to the high pointing accuracies required by antennae providing the desired coverage on the earth's surface. It is thus prudent for designers to avoid the regions of chaotic instability via parameter design, however, a successful control methodology would allow designers to use spacecraft parameters (desired for other requirements) that would normally render the spacecraft susceptible to chaotic instabilities. At present there has been no results obtained for the control of chaotic instabilities in spacecraft.

Control of chaotic motion is a very new field of research, however, a vast array of different control techniques have been employed, over this decade, to suppress or manipulate chaotic instabilities. Lindner and Ditto [9] present a comprehensive review of these techniques. Blazejczyk et al. [10] also describe a variety of methods used for the control of chaos in mechanical systems. The present research uses two methods for the control of chaotic vibrations in a simplified model of a spinning spacecraft. The first method is a Recursive Proportional Feedback (RPF) method derived by Rollins et al. [11] and is an extension of the Occasional Proportional Feedback (OPF) technique. Both these methods are derived from the renowned model-independent technique proposed by Ott Grebogi and Yorke (OGY) [9]. Hunt [12] and Roy et al. [13] give two examples of the employment of the OPF method in experimental systems and Parmananda et al. [14] has used the RPF method to control the dissolution of the anode in an electrochemical cell. The second technique used in this paper is a continuous Delayed feedback method devised by Pyragas [15, 16]. Both methods require no prior knowledge of the system dynamics.

For the purpose of the present analysis, a simple model of spinning spacecraft with a circumferential nutational damper is chosen and no linearisation of the equations of motion has been performed. Such a model is a simplification of a dual spin spacecraft in that platform and nonprincipal axis rotations are not considered. A circumferential damper was chosen over an axial damper to allow simplification of the problem to one plane as well as because of its effectiveness in operation over a wider range of nutation angles as found by Cochran and Thompson [17]. Chaotic motion has been previously found in this simplified model when the spacecraft is subjected to an external periodically varying torque by Meehan and Asokanthan [18]. Such a torque, in practice, may arise in the platform of a dual-spin spacecraft under malfunction of the control system causing rotor driver fluctuations and hence periodic torquing of the platform. A similar situation may also arise in a dual-spin spacecraft during spin-up of an unbalanced rotor or from vibrations in appendages. Two control methods will be applied to the system, under the conditions causing chaotic motion, to eliminate instabilities.

This paper first gives a simplified description and formulation of the equations of motion governing the dynamics of the system. A summary of the results obtained describing the presence of chaotic instabilities is then described. Also an outline of each control method and its design implementation is presented. Numerical simulation results are shown and the effectiveness of each control method on this model is compared and contrasted.

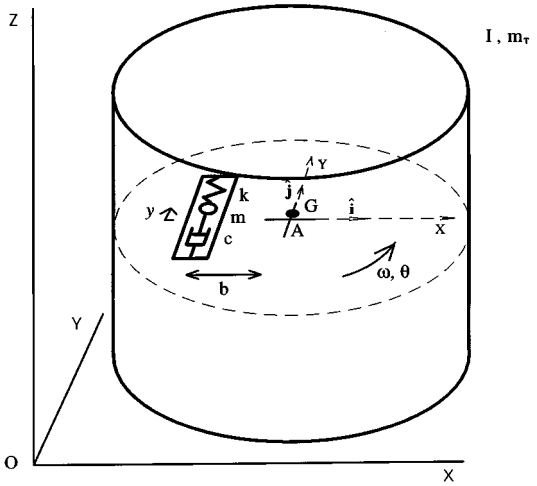

Figure 1. Spinning spacecraft with internal spring-mass-damper configuration.

2. Equations of Motion and Stability Analysis

The system under investigation consists of a rigid body rotating at angular velocity ω with an internal energy dissipater in the form of a spring-mass-dashpot as illustrated in Figure 1. The degrees-of-freedom of the system, y and θ describe the displacement of the damper mass and rotation of the system about A (or G), respectively. The damper is centred on the body fixed X-axis and has a point mass of m that moves along an axis parallel to the Y-axis at a distance b from A. The spring constant is k and the dashpot has damping constant c. The system rotates about its centre of mass at point G which coincides with A when $y = 0$. Note that the position of A with respect to the motionless centre of mass G and the instantaneous moment of inertia of the system about A, vary with the position of the damper mass. The system is considered to have a total mass m_T, moment of inertia I about the Z-axis when $y = 0$. The system is also considered to be subjected to a combination of external torques M, composed of an excitational time varying torque M_E and a control torque M_C such that $M = M_E + M_C$.

The equations of motion for the system may be obtained using Lagrange's Equations with dissipation. Grubin [19] has derived similar equations of motion for "A Translating Point Mass on a Vehicle Moving in Two Dimensions" using the generalised angular momentum equation derived by himself previously [20]. A similar generalisation of the kinetic energy equation has been derived by Meehan and Asokanthan [21] which allows the kinetic energy of a system of particles to be calculated with respect to an arbitrary frame of reference in the system, having an arbitrary motion. Meehan and Asokanthan [18, 21] have derived the equations for this model previously in dimensional form. These equations may be transformed to a nondimensional form using the following dimensionless quantities:

$$\tau = \Omega t, \quad \hat{y} = \frac{(1-\mu)y}{b}, \quad \hat{\omega} = \frac{\omega}{\Omega}, \quad \hat{I} = \frac{(1-\mu)I}{mb^2}, \quad \hat{c} = \frac{c}{m(1-\mu)\Omega},$$
$$\hat{k} = \frac{k}{m(1-\mu)\Omega^2}, \quad \hat{M} = \frac{(1-\mu)M}{mb^2\Omega^2}, \quad \hat{E} = \frac{(1-\mu)E}{mb^2\Omega^2}, \quad \mu = \frac{m}{m_T}, \tag{1}$$

where Ω and τ denote the frequency of the time varying torque M and the nondimensional time, respectively, while E denotes the total mechanical energy of the system. The super-

script ($\hat{}$) denotes a nondimensional parameter. Using Equations (1), the dimensionless total mechanical energy of the system may be derived as

$$\hat{E} = \frac{1}{2}\,[\hat{I} + \hat{y}^2]\hat{\omega}^2 + \frac{1}{2}\,\hat{y}'^2 + \frac{1}{2}\,\hat{k}\hat{y}^2 - \hat{y}'\hat{\omega}. \tag{2}$$

The dimensionless equations of motion are also derived as

$$[\hat{I} + \hat{y}^2]\hat{\omega}' + 2\hat{y}\hat{y}'\hat{\omega} - \hat{y}'' = \hat{M}(\tau), \tag{3}$$

$$\hat{y}'' + \hat{c}\hat{y}' + \hat{k}\hat{y} - \hat{\omega}^2\hat{y} - \hat{\omega}' = 0, \tag{4}$$

where $(\,)'$ denotes differentiation with respect to the dimensionless time τ. Equation (3) is the simplified Euler's equation representing the dynamics of a spinning spacecraft with circumferential nutational damper. The coefficient of $\hat{\omega}'$ in Equation (3) represents the instantaneous moment of inertia of the system about G while the terms involving $\hat{y}'$ and $\hat{y}''$ represent the moments arising from the Coriolis and other inertia forces with respect to G. Equation (4) represents the acceleration-force balance of the spring mass damper system where the last two terms characterise the effects of the centrifugal and angular accelerations, respectively. It may be noted that these two equations completely describe the system dynamics. In this case, the system is of order five since $\hat{M}$ is assumed to vary periodically with time and state equation described by $\hat{\theta}' = \hat{\omega}$ is trivial. It may also be observed that Equations (3) and (4) are coupled through three nonlinear terms resulting from the dynamic effects of the damper point mass. The subsequent analysis will investigate the dynamical response of this system to a combination of external torques $\hat{M}$, composed of an excitational time varying torque $\hat{M}_E$ and a control torque $\hat{M}_C$ such that $\hat{M} = \hat{M}_E + \hat{M}_C$. To gain an initial understanding of the dynamical behaviour, a stability analysis is performed.

The stability of the system was examined by considering the equations of motion (3) and (4). These equations may be rearranged and transformed into three nonlinear state equations

$$\begin{aligned} X_1' &= X_2, \\ X_2' &= \beta(X_1)[\alpha(X_1)\chi(\mathbf{X}) + \delta(\mathbf{X})], \\ X_3' &= \beta(X_1)[\chi(\mathbf{X}) + \delta(\mathbf{X})], \end{aligned} \tag{5}$$

where

$$\mathbf{X} = [X_1 \;\; X_2 \;\; X_3]^T = [\hat{y} \;\; \hat{y}' \;\; \hat{\omega}]^T, \quad \alpha(X_1) = (\hat{I} + X_1^2), \quad \beta(X_1) = (\hat{I} + X_1^2 - 1)^{-1},$$
$$\chi(\mathbf{X}) = -\hat{c}X_2 + (X_3^2 - \hat{k})X_1, \quad \delta(\mathbf{X}) = \hat{M} - 2X_1X_2X_3.$$

Note that the state equation described by $\hat{\theta}' = \hat{\omega}$ is trivial in this case. The critical points for the homogenous system were then found by setting $[\hat{y}' \;\; \hat{y}'' \;\; \hat{\omega}']^T = [0 \;\; 0 \;\; 0]^T$ and $\hat{M} = 0$ to obtain three lines of equilibrium described by

$$[\hat{y} \;\; \hat{\omega}]^T = [0 \;\; \bar{\omega}]^T, \left[\bar{y} \;\; \sqrt{\hat{k}}\right]^T, \left[\bar{y} \;\; -\sqrt{\hat{k}}\right]^T, \tag{6}$$

where $\bar{\omega}$ and $\bar{y}$ indicate infinite sets of real values or lines in equilibrium phase space. Once the initial conditions of the system are prescribed these lines reduce to a finite number of equilibrium points. The equilibrium configuration thus depends on the initial conditions of

the system. The stability of these equilibrium lines has been investigated previously by Meehan and Asokanthan [18, 21]. The stability analysis revealed that the first equilibrium line described by $[\hat{y} \;\; \hat{\omega}]^T = [0 \;\; \bar{\omega}]^T$ is stable if

$$\hat{k} - \bar{\omega}^2 > 0 \quad \text{and} \quad \hat{I} - 1 > 0 \tag{7}$$

and the other two equilibrium lines described by $[\hat{y} \;\; \hat{\omega}]^T = \left[\bar{y} \;\; \pm\sqrt{\hat{k}}\right]^T$ are stable if

$$\hat{I} - 1 + \bar{y}^2 > 0. \tag{8}$$

It may be noted that for any given set of initial conditions, the equilibrium lines $\bar{\omega}$ and $\bar{y}$ described in Equation (6) would reduce to the possible critical points $\bar{\omega}^*$ and $\pm\bar{y}^*$, respectively, due to the symmetry of displacement of the mass damper and rotation of the body, where $\bar{\omega}^*$ and $\bar{y}^*$ indicate single values. The relationship of the equilibrium configuration with initial conditions may be derived considering conservation of angular momentum of the system as described in Appendix A. From this analysis the sign of the first of these equilibrium points $\bar{\omega}^*$ is found to be directly dependent on the sign of the initial angular momentum of the system. It may also be noted that the stability of the equilibrium points in the direction of the equilibrium line may be determined to be stable for the conditions described by Equations (7) and (8) using Lyapunov's direct method, with the total mechanical energy of the system as a Lyapunov function.

It is also noticed that the stability configuration of the system may be determined by the angular momentum and initial energy of the system. Thus if the system has no external torque applied ($\hat{M} = 0$), it is dissipative and the behaviour of the system can be predicted using Equations (2), (6–8). For initial conditions such that the initial angular momentum in the system is less than that described by the system having only an angular rotation of $\hat{\omega}^2 = \hat{k}$ the system is attracted to the stable condition defined by the first equilibrium state in Equation (6) of a constant angular velocity $\bar{\omega}$ and no damper mass deflection. Under these conditions, by considering Equation (2), there is not enough energy within the system for the latter two equilibrium lines described by Equation (6)to be approached in phase space since the damper acts to dissipate energy always. The energy associated with any initial damper mass displacement is partly dissipated in the damper and also transferred to rigid body rotational energy via an increase in $\hat{\omega}$ so as to conserve total angular momentum. For initial conditions such that the angular momentum in the system is greater than that described by the system having only an angular rotation of $\hat{\omega}^2 = \hat{k}$, the first stability condition described by Equation (7) is violated, so that either one of the latter two equilibrium lines described by Equation (6) become the dominant attractor depending on the sign or direction of $\bar{\omega}^*$. In this case, any initial rigid body rotational energy that is lost is partly dissipated and partly stored in a displacement of the damper mass $\bar{y}^*$ such that angular momentum is conserved again. In each case, the system acts in such a way as to conserve angular momentum but minimise final energy. Such a heuristic argument is similar to that which describes why a semirigid body with internal energy dissipation is stable only when spinning about its major axis [22].

The symmetrical properties of the spring mass damper allow the possibility of two stable equilibrium points; in this case corresponding to positive and negative displacements of the damper mass $\pm\bar{y}^*$. This characteristic of two stable equilibrium points is similar to that described by a two-well potential problem. The system will be attracted to either one of the equilibrium points depending on the initial conditions and there will be a region in phase space where this dependence will be highly sensitive to small changes. This characteristic

can become significant to the dynamics when an external sinusoidal torque is applied to the system. As has been found with many systems of this type, Meehan and Asokanthan [21] found an external sinusoidal torque applied to the body about a perpendicular axis through A, induces the system to jump chaotically between the two stable equilibrium points. Evidence is also presented, indicating that the onset of chaotic motion was characterised by period doubling as well as intermittency. These results are of importance to spacecraft designers as any instabilities in the attitude dynamics of a spacecraft could have disastrous affects on its normal operation. For example, chaotic motion in the attitude motion of a communication satellite would be seriously detrimental to the high pointing accuracies required by antennas providing the desired coverage on the earth's surface. It is thus prudent for designers to avoid the regions of chaotic instability via parameter design. However, a successful control methodology would allow designers to use spacecraft parameters (desired for other requirements) that would normally render the spacecraft susceptible to chaotic instabilities.

3. Control Methods

The control methods used in this paper are model independent methods that exploit the universal characteristics of chaotic vibrations. Owing to this property, the methods employed are able to detect the presence of chaotic motion, switch on the control when required and switch off once it is no longer required. For this system, the aim is to stabilise the desired state $[\hat{y} \quad \hat{y}' \quad \hat{\omega}]^T = [0 \quad 0 \quad \omega_{\text{ref}}]^T$, which corresponds physically to the desired operation conditions for a satellite of constant rotation rate and no nutation or precession. In order to achieve simplicity in design of the control mechanism, the angular velocity of the spacecraft $\hat{\omega}$ is chosen as the sensor variable and the control actuator is considered to be a torque applied to the spacecraft $\hat{M}_C$. Such a control torque could be considered to be applied using thrusters or an external rotor in a dual-spin satellite. Thus, when the controlled system is being perturbed by an excitational periodically varying torque, it is considered to be subjected a combination of applied torques $\hat{M} = \hat{M}_E + \hat{M}_C$ about the spinning axis. Due to practical constraints a torque limitation of $M_{\max}$ is chosen for the control actuator.

3.1. Continuous Delayed Feedback Control

The first control method implemented on the present model was first proposed by Pyragas as a method of time continuous control. This method is based on the construction of a special form of a time continuous perturbation which does not change the form of a desired unstable periodic orbit or fixed point. The control may be applied to any number of the system state space equations in the form:

$$\dot{\mathbf{X}} = \mathbf{F}(\mathbf{X}, p) + \hat{\mathbf{u}}_i C(\tau),$$

where $\dot{\mathbf{X}} = \mathbf{F}(\mathbf{X}, p)$ represents the state space equations of motion, $\hat{\mathbf{u}}_i$ is a unit vector in the direction of the ith variable and the control signal is sensitive to the ith variable in the form

$$C(\tau) = K[x_i(\tau - \Delta) - x_i(\tau)],$$

where Δ is the delay time and x_i is the ith variable. Note that $C(\tau) = 0$ when $x_i(\tau - \Delta) = x_i(\tau)$. This occurs when the system is settled on a limit cycle of period Δ. Control design is performed simply via adjustment of the delay Δ to the period of the desired unstable periodic

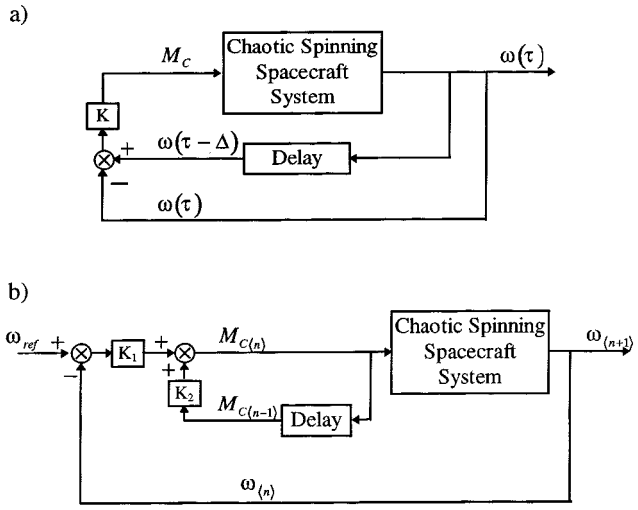

Figure 2. Block diagram of control methods: (a) delayed feedback and (b) recursive proportional feedback (RPF).

orbit and weight K of the feedback. Recently, Barrett [23] has presented analytical results describing a method of determining the required feedback gain K. It may be noted that only sufficient conditions for stability are employed using this method and in practice adjustment of the feedback K is required for more effective controller performance. Typically, K is set low and gradually increased until desired stabilisation occurs [15, 16].

For the present model, a suitable choice for control parameters is $x_i \equiv \hat{\omega}$ such that after introducing a torque limitation $M_{\max}$ the control law may be given by

$$\hat{M}_C(\tau) = \left\{ \begin{array}{ll} C(\tau) & |\hat{M}_C(\tau)| < M_{\max} \\ M_{\max}, & \hat{M}_C(\tau) > M_{\max} \\ -M_{\max}, & \hat{M}_C(\tau) < -M_{\max} \end{array} \right\}, \quad C(\tau) = K[\hat{\omega}(\tau - \Delta) - \hat{\omega}(\tau)].$$

The block diagram of this system is seen in Figure 2a. For the present model, the aim is to stabilise a fixed point so that in practice the delay Δ is chosen to be smaller than the forcing period. Also the initial control actuation conditions described by

$$|\hat{\omega}| < \frac{\hat{I}\hat{k}}{\hat{h}_G} \quad \text{and} \quad \hat{y}\hat{y}' < 0 \tag{9}$$

are employed so that the equilibrium state described by $[\hat{y} \;\; \hat{y}' \;\; \hat{\omega}]^T = [0 \;\; 0 \;\; \bar{\omega}^*]^T$ is stabilised rather than a limit cycle about the equilibrium states $[\hat{y} \;\; \hat{y}' \;\; \hat{\omega}]^T = \left[\pm\bar{y}^* \;\; 0 \;\; \pm\sqrt{\hat{k}}\right]^T$. The first condition described in Equation (9) is devised using the first stability condition described by Equation (7) and the result describing the equilibrium point, $\bar{\omega}^*$, derived in Appendix A. The second condition described in Equation (8) ensures that the control is activated when the movement of the damper mass, $\hat{y}$, is towards the desired fixed point position $\hat{y} = 0$.

3.2. RPF Control

The second method, a Recursive Proportional Feedback (RPF) is an extension of the Occasional Proportional Feedback (OPF) technique [12]. This method has been derived from

the renowned technique proposed by Ott Grebogi and Yorke (OGY) [9] which is model-independent and goal-oriented. Like the OPF method, the RPF is useful in highly dissipative systems where dynamics exhibits a nearly one-dimensional return map. RPF has an extra derivative-like term as compared to OPF that adds greater stability for control. The method, however, can only be applied to discrete mappings of a dynamical system.

The control method provides small perturbations to a system parameter which is proportional to the error from the desired output of a sensor variable for the system. For a discrete mapping, the control law for the nth iterate is given by

$$\delta p_n = \left\{ \begin{array}{cc} K_1 \delta x_n + K_2 \delta p_{n-1} & |K_1 \delta x_n| \leq \delta p_{\max} \\ 0 & |K_1 \delta x_n| > \delta p_{\max} \end{array} \right\}, \tag{10}$$

where δp_n defined as $p_n - p_0$ is the relative control parameter perturbation while p_n, p_0 denote the control parameter for the nth iterate and the uncontrolled value of the control parameter, respectively. The relative sensor displacement, δx_n from desired fixed point x_f is defined as $x_n - x_f$ where x_n signifies the sensor value at the nth iterate. Also, $|K_1 \delta x_n| \leq \delta p_{\max}$ defines a region or "window" in phase space around the desired fixed point where linear approximation is valid and $K_2 \delta p_{n-1}$ is a "derivative-like" term which can add stability and optimise the control method.

Generally, the mapping frequency is chosen to be the same as an external forcing frequency or a natural frequency of the system. Rollins et al. [11] provides a method of determination of feedback gains K_1 and K_2 via experimentation and measurement from one-dimensional return maps of the controlled system. This method assumes linear behaviour of the system about the fixed point and is valid for small control perturbations. In practice, adjustment of the two feedback gains K_1 and K_2 as well as adjustment of the "window" size $\delta p_{\max}$ is required for more effective controller performance. Typically, the procedure involves tuning gains K_1 and K_2 with a small "window" $\delta p_{\max}$, then gradually increasing the size and adjusting the gains for optimal controller performance.

For the present model a suitable choice for control parameters is

$$p_n \equiv \hat{M}_{C\langle n \rangle}, \quad p_0 \equiv 0, \quad x_n \equiv \hat{\omega}_{\langle n \rangle}, \quad x_f \equiv \omega_{\text{ref}},$$

such that

$$\delta p_n \equiv \hat{M}_{C\langle n \rangle}, \quad \delta x_n \equiv \hat{\omega}_{\langle n \rangle} - \omega_{\text{ref}} \quad \text{and} \quad \delta p_{\max} \equiv M_{\max},$$

where $(\,)_{\langle n \rangle}$ is the nth map iterate. Therefore, the control law may be given by

$$\hat{M}_{C\langle n \rangle} = \left\{ \begin{array}{cc} K_1(\hat{\omega}_{\langle n \rangle} - \omega_{\text{ref}} + K_2 \hat{M}_{C\langle n-1 \rangle} & |\hat{M}_{C\langle n \rangle}| \leq M_{\max} \\ 0 & |\hat{M}_{C\langle n \rangle}| > M_{\max} \end{array} \right\}.$$

The block diagram of this system is seen in Figure 2b. In practice, the control design is implemented on a continuous system by holding the control constant for each period of the excitation torque.

4. Numerical Simulations

In order to investigate the effect of the control methods upon the chaotic dynamics of the system, numerical integration of Equations (2) and (3) was performed while the system is

subjected to a excitational time varying torque $\hat{M}_E$. All numerical simulations were performed on a Sun SPARC Station IPX using DYNAMICS, written by Nusse and Yorke. The fourth and fifth order Runge–Kutta routine was used for numerical integration. Various tools were used to examine the effect of the control methods upon nonlinear phenomena including the time history, bifurcation diagrams of Poincaré maps and Lyapunov Exponents. The Lyapunov spectrum of exponents was calculated using the algorithm derived by Wolf et al. [24] and iterated at least 1000 forcing periods. Renormalisation was performed at 1/2 forcing period.

The equations of motion in the state space form of Equations (4) were used for the integration with the combination of external torques described by $\hat{M} = \hat{M}_E + \hat{M}_C$ where $\hat{M}_E = \hat{M}_E \cos\tau$. The parameters of the spinning spacecraft with circumferential nutational damper were chosen to be similar to that of INTELSAT II or III being $m = 0.3$ kg, $b = 1$ m, $k = 0.2$ N/m, $\mu = 0.01$, $I = 100$ kg m^2, and the numerical integrations began from the initial conditions described by $[y \;\; \dot{y} \;\; \omega]^T = [0 \;\; 0 \;\; 0.821 \text{ rad/s}]^T$. The damping constant and excitation torque frequency was chosen to be $c = 0.002$ Ns/m and $\Omega = 0.05$ rad/s, respectively. The nondimensional parameters for the system are thus given by $\hat{c} = 0.13468$, $\hat{k} = 269.36$ and $\hat{I} = 330$ and the numerical integrations began from the initial conditions described by $[\hat{y} \;\; \hat{y}' \;\; \hat{\omega}]^T = [0 \;\; 0 \;\; 16.42]^T$. For these parameter values it is noted from the conditions described by Equations (14) and (15) and the results obtained in Appendix A that the equilibrium points $[\hat{y} \;\; \hat{\omega}]^T = [0 \;\; \bar{\omega}^*]^T$ are stable for $-16.33 < \hat{\omega} < 16.33$ while the other equilibrium points $[\hat{y} \;\; \hat{\omega}]^T = [\pm 0.396 \;\; \pm 16.4122]^T$ are always stable.

Firstly, the characteristic nonlinear phenomena in the open loop system were investigated primarily while varying the amplitude of the excitation torque, $\hat{M}_E$. An intermittent route to chaos was found for the system using the parameters above. The intervals of intermittent chaos was found to increase with excitation torque amplitude and at $\hat{M}_E = 1.584$ fully developed chaos is present as seen in Figures 3a and 3b, respectively, via phase space and Poincaré map. The time history and power spectrum also confirmed these results. The characteristic Lyapunov exponents were calculated to be $[0.94 \;\; 0.0 \;\; 0.0 \;\; -1.9] \times 10^{-2}$ with the positive exponent confirming chaotic motion. The correlation dimension of the system was calculated from the Poincaré map to be $D_C = 2.482$. The closeup portion of the Poincaré map shown in Figure 3b shows a one-dimensional map behaviour, supporting the use of the RPF method for control of the chaotic behaviour. Consequently, it was of interest to investigate the effectiveness of the two control methods on the system while it is subjected to the same excitation torque amplitude, $\hat{M}_E = 1.584$.

Figures 4 to 6 show the effect of each control method via time histories of the control torque, damper mass position and angular velocity of the body. In each case, the control loop is manually closed after a short interval as indicated on the diagrams so that a comparison of the open loop and closed loop systems can be made. The control torque limitation is also chosen in each case to be $M_{\max} = 10^3$.

Figures 4a–c show the effect of applying the delayed feedback method to system while it is behaving chaotically. Control is achieved via adjustment of the control parameters as described in Section 3.1 to $K = 3.3 \times 10^3$ and $\Delta = 0.25$. A large control torque is activated almost immediately after the control loop is closed. The control is effective in eliminating the large amplitude instability down to a small oscillation about a constant angular velocity as seen in Figure 4c.

Figures 5a–c show the effectiveness of the RPF control method under the same conditions. The control parameters are tuned as described in Section 3.2 to be $K_1 = 52.8$ and $K_2 = 0.02$.

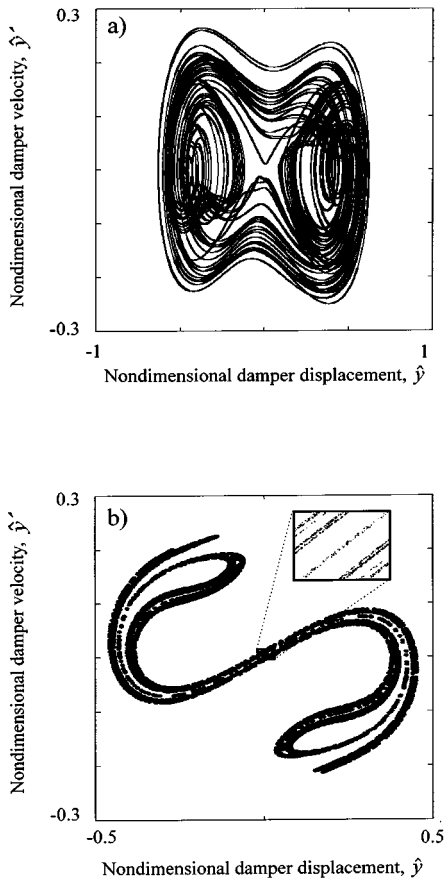

Figure 3. Numerical simulation for an excitational torque amplitude of showing chaotic motion via (a) phase space and (b) Poincaré map.

For comparison with the continuous delayed feedback method, the desired reference angular velocity is chosen to be $\omega_{\text{ref}} = 16.41$. In comparison with the delayed feedback method, the control torque amplitude is an order of magnitude smaller; however, the amplitude of the final oscillation in angular velocity is larger. Optimisation of control parameters can decrease this amplitude however the discreteness of the control method is a limitation in the reduction of this final amplitude.

Figures 6a–c show the effectiveness of the RPF control method under the same conditions but with the desired reference angular velocity chosen to be $\omega_{\text{ref}} = 4$. These conditions represent a large decrease in angular velocity from initial conditions as required during despin of a dual-spin spacecraft. Initially, a much larger control torque amplitude is required, when compared to the previous cases, since the desired final state requires a change in angular momentum. The method is seen to be effective in eliminating the chaotic instability and reaching the desired final state quickly.

To test the robustness of each control technique, the excitational torque amplitude was varied and a bifurcation diagram of the Lyapunov spectrum of the system was obtained for the open loop and closed loop cases. Figures 7a–c illustrate these results. The open loop case is depicted in Figure 7a. Chaotic motion, indicated by a positive maximal Lyapunov exponent,

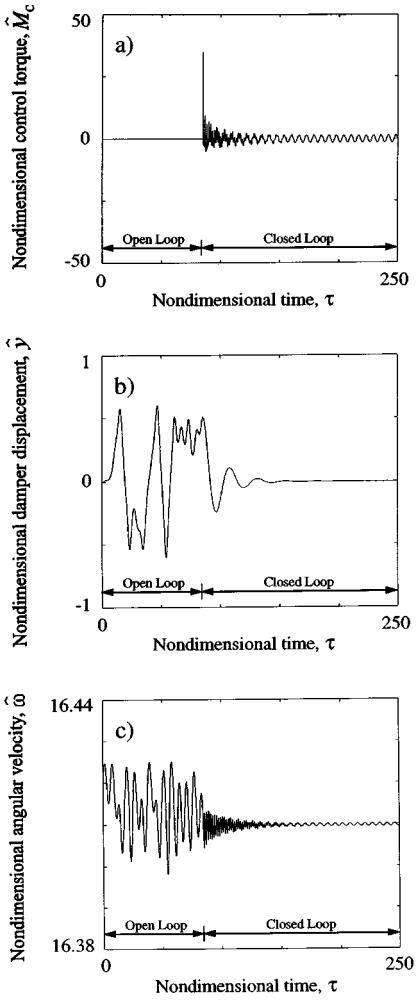

Figure 4. Numerical simulation for an excitational torque amplitude of using delayed feedback showing elimination of chaotic motion via time histories of (a) control torque, (b) damper displacement, and (c) angular velocity.

is present for excitational torque amplitudes $\hat{M}_E > 1.33$. The uncertainty in the Lyapunov exponents is related to the intermittent nature of the chaotic behaviour. The closed loop results for the delayed feedback and RPF methods are shown in Figures 7b and 7c, respectively. In each case, the control parameters were chosen to be the same as previously mentioned values. The maximal Lyapunov exponent is reduced to zero for the same range of excitational torque amplitude as the open loop case indicating that the chaotic instability has been quenched in both cases. The zero maximal Lyapunov exponent obtained at the fixed point is due to the zero eigenvalue with eigenvector in the direction of the equilibrium line $\bar{\omega}$. Bifurcation diagrams of time history confirmed that the desired equilibrium point was stabilised in each case.

Although both control methods were successful in eliminating the chaotic instabilities in the present model for a range of excitation torque amplitudes a number of advantages and limitations were noticed. The delayed feedback method was seen to be more effective in suppressing the resultant oscillations in angular velocity. This is primarily due to the con-

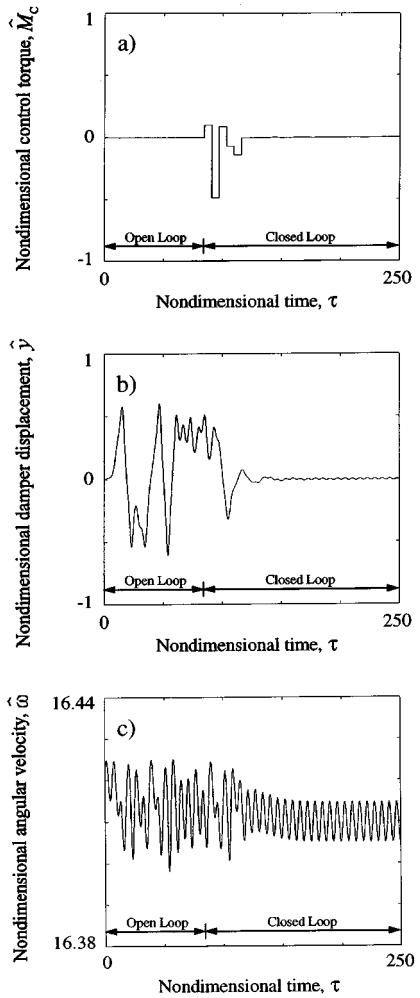

Figure 5. Numerical simulation for an excitational torque amplitude of using recursive proportional feedback (RPF) and showing elimination of chaotic motion via time histories of (a) control torque, (b) damper displacement, and (c) angular velocity.

tinuous nature of the method. The discrete nature of the RPF method could lead to some other serious limitations. As has been mentioned by Blazejczyk et al. [10], this method can only stabilise those periodic orbits whose maximal Lyapunov exponent is small compared to the reciprocal of the time interval between the parameter changes. Since the corrections of the control torque are rare and small, any noise fluctuation leads to occasional outbursts of the system into a region far from the desired periodic orbit. However, the RPF method is simple in design, requiring only one sensor, low control torques and would be ideal for use on a spacecraft configuration with torque thrusters as actuators. The method also has the added flexibility over the delayed feedback method of control to any desired angular velocity ω_{ref}. In contrast, the delayed feedback method requires sensor input from three state variables due to required initial actuation conditions and the final angular velocity is determined by the total angular momentum of the system. The continuous nature of the method would require the use of an external rotor or momentum wheel for torque actuation rather than thrusters. In practice,

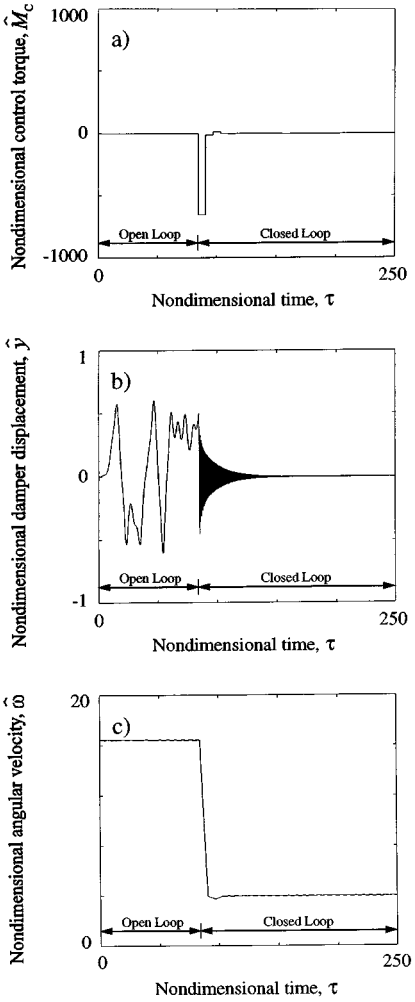

Figure 6. Numerical simulation for an excitational torque amplitude of using recursive proportional feedback (RPF) and showing elimination of chaotic motion via time histories of (a) control torque, (b) damper displacement, and (c) angular velocity.

both techniques would be simple to implement on a spacecraft as they require very little or no prior knowledge of the system dynamics.

5. Conclusions

Numerical simulations have shown the effectiveness of two control techniques in eliminating chaotic instabilities in a spinning spacecraft with internal energy dissipation when it is perturbed by an external periodically varying torque. A typical spacecraft parameter configuration is investigated and is found to exhibit chaotic motion for a range of rotor torque perturbation amplitude and frequency. A similar situation, in practice, may arise in the platform of a dual-spin spacecraft under malfunction of the control system or during spin-up of an unbalanced rotor or due to appendage vibrations. The control techniques are then successfully employed to eliminate the instability. The robustness of each technique is shown for a range of excitation

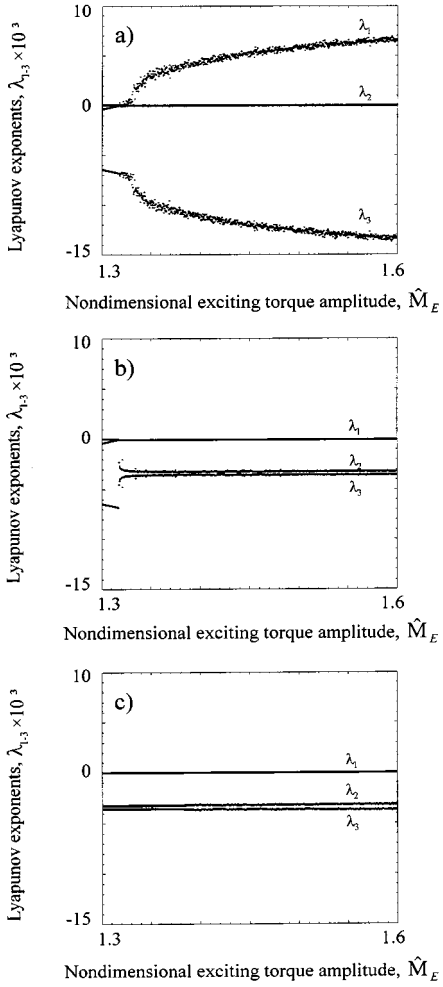

Figure 7. Bifurcation diagrams of Lyapunov spectrum of exponents for (a) open loop system, (b) closed loop system with delayed feedback, and (c) closed loop system with recursive proportional feedback (RPF).

torque amplitudes. From a practical point of view, chaotic instabilities could introduce uncertainties and irregularities into a spacecraft's attitude and subsequently could have disastrous affects on its operation. It is thus important for spacecraft designers to be able to avoid these instabilities by employing the control techniques investigated in this paper. Each technique is outlined and the effectiveness on this model compared and contrasted. In practice, both techniques would be simple to implement on a spacecraft as they require very little or no prior knowledge of the system dynamics.

Acknowledgment

The authors gratefully acknowledge the support of the members of the Applied Chaos Laboratory for their enlightening discussions and ideas while visiting the School of Physics at the Georgia Institute of Technology.

Appendix A: Derivation of Equilibrium Points

The total angular momentum of the system about the centre of mass G is given by

$$h_G = [I + m(1-\mu)y^2]\omega - mb\dot{y}.$$

This may be expressed in nondimensional form as

$$\hat{h}_G = (\hat{I} + \hat{y}^2)\hat{\omega} - \hat{y}', \quad \text{where} \quad \hat{h}_G = \frac{(1-\mu)h_G}{mb^2\Omega}.$$

For the condition of no external torque on the system, the principle of conservation of angular momentum may be applied in the form

$$\hat{h}_{Gi} = \hat{h}_{Gf},$$

where $\hat{h}_{Gi}$ and $\hat{h}_{Gf}$ are the initial and final angular momenta of the system, respectively. By substituting the final conditions described by the equilibrium point $[\hat{y} \;\; \hat{\omega}]^T = [0 \;\; \bar{\omega}^*]^T$, the above equation yields

$$\bar{\omega}^* = \frac{\hat{h}_{Gi}}{\hat{I}}.$$

This result reveals that for this equilibrium point, the sign or direction of the final angular velocity of the system, $\bar{\omega}^*$, is the same as the sign of the initial angular momentum h_{Gi}. For the final conditions described by the equilibrium points $[\hat{y} \;\; \hat{\omega}]^T = \left[\bar{y}^* \;\; \pm\sqrt{\hat{k}}\right]^T$, the above equation yields

$$\pm\bar{y}^* = \pm\sqrt{\frac{\hat{h}_{Gi}}{\pm\sqrt{\hat{k}}} - \hat{I}}.$$

This result also reveals that for these equilibrium points the sign or direction of the final angular velocity of the system $\pm\sqrt{\hat{k}}$ must be of the same sign as that of the initial angular momentum $\hat{h}_{Gi}$ in order that a real value for $\pm\bar{y}^*$ may be obtained.

References

1. Lukich, M. S. and Mingori, D. L., 'Attitude stability of dual-spin spacecraft with unsymmetrical bodies', *Journal of Guidance, Control and Dynamics* **8**(1), 1985, 110–117.
2. Agrawal, Brij. N., 'Effects of asymmetries in the rotor and flexible joint of a dual-spin spacecraft', *Journal of Spacecraft and Rockets* **11**(9), 1974, 611–612.
3. Van Doorn, J. E. and Asokanthan, S. F., 'Attitude stability of an asymmetric spacecraft', in *Proceedings of the IEAust. Eighth National Space Engineering Symposium*, NCP No. 93/7, Brisbane, 20–21 September 1993, pp. 309-317.
4. Moon, F. C., *Chaotic and Fractal Dynamics*, Wiley, New York, 1992.
5. Holmes, P. J. and Marsden, J. E., 'Horseshoes and Arnold diffusion for Hamiltonian systems on Lie groups', *Indiana University Mathematics Journal* **32**(2), 1983, 273–309.
6. Koiller, J., 'A mechanical system with a 'wild' horseshoe', *Journal of Mathematical Physics* **25**(5), 1984, 1599–1604.
7. Piper, G. E. and Kwatny, H. G., 'Complicated dynamics in spacecraft attitude control systems', *Journal of Guidance, Control and Dynamics* **15**(4), 1992, 825–831.

8. Gray, G. L., Kammer, D. C., and Dobson, I., 'Detection of chaotic saddles in an attitude maneuver of a spacecraft containing a viscous damper', *Advances in the Astronautical Sciences* **82**(1), 1993, 167–184.
9. Lindner, J. F. and Ditto, W. L., 'Removal, suppression and control of chaos by nonlinear design', *Applied Mechanics Review* **48**(12), pt. 1, 1995, 795–808.
10. Blazejczyk, B., Kapitaniak, T., Wojewoda, J., and Brindley, J., 'Controlling chaos in mechanical systems', *Applied Mechanics Review* **46**(7), 1993, 385–391.
11. Rollins, R. W., Parmananda, P., and Sherard, P., 'Controlling chaos in highly dissipative systems: A simple recursive algorithm', *Physical Review E* **47**, 1993, R780–R783.
12. Hunt, E. R., 'Stabilising high periodic orbits in a chaotic system: The diode resonator', *Physical Review Letters* **67**, 1991, 1953–1955.
13. Roy, R., Murphy, T. W., Jr., Maier, T. D., Gills, Z., and Hunt, E. R., 'Dynamical control of a chaotic laser: Experimental stabilisation of a globally coupled system', *Physical Review Letters* **68**, 1992, 1259–1262.
14. Parmananda, P., Sherard, P., Rollins, R. W., and Dewald, H. D., 'Control of chaos in an electrochemical cell', *Physical Review E* **47**, 1993, R3003–R3006.
15. Pyragas, K., 'Continuous control of chaos by self-controlling feedback', *Physics Letters A* **170**, 1992, 421–428.
16. Pyragas, K. and Tamasevicius, A., 'Experimental control of chaos by delayed self-controlling feedback', *Physics Letters A* **180**, 1993, 92–102.
17. Cochran, J. E., Jr. and Thompson, J. A., 'Nutation dampers vs precession dampers for asymmetric spacecraft', *Journal of Guidance and Control* **3**, 1980, 22–28.
18. Meehan, P. A. and Asokanthan, S. F., 'Chaotic motion in a rotating body with internal energy dissipation', in *Nonlinear Dynamics and Stochastic Mechanics*, W. H. Kliemann, W. F. Langford, and N. S. Namachchivaya (eds.), Fields Institute Communications, Vol. 9, AMS, Providence, RI, 1996, pp. 175–202.
19. Grubin, C., 'Dynamics of a vehicle containing moving parts', *ASME, Journal of Applied Mechanics* **29**, 1962, 486–488.
20. Grubin, C., 'On generalisation of the angular momentum equation', *Journal of Engineering Education* **51**(3), 1960, 237–238, 255.
21. Meehan, P. A. and Asokanthan, S. F., 'Chaotic motion in a spinning spacecraft with circumferential nutational damper', *Nonlinear Dynamics* **12**, 1997, 69–87.
22. Hughes, P. C., *Spacecraft Attitude Dynamics*, Wiley, New York, 1986.
23. Barrett, M. D., 'Continuous control of chaos', *Physica D* **91**, 1996, 340–348.
24. Wolf, A., Swift, J. B., Swiruney, H. L., and Vasano, J. A., 'Determining Lyapunov exponents from a time series', *Physica D* **16**, 1985, 285–317.